Advanced Materials Research Vol. 59 (2009) pp 198-203
online at http://www.scientific.net

Stress state, texture, phase and morphology analysis of thin graded W/Cu coatings on tungsten and their thermal behaviour in fusion application

A. Herrmann [1, a], M. Balden[1,b], M. Rasiński [1,2,c] and H. Bolt[1,3,d]

[1]Max-Planck-Institut für Plasmaphysik, Bolzmannstraße 2, D-85748 Garching

[2]Wydzial Inzynierii Materialowej, Warsaw University of Technology, 02-507 Warszawa

[3]Forschungszentrum Jülich GmbH, D-52425 Jülich, Germany

[a]aurelia.herrmann@ipp.mpg.de, [b]martin.balden@ipp.mpg.de, [c]mrasin@o2.pl, [d]harald.bolt@ipp.mpg.de

Keywords: thin graded W/Cu coating, stress, phase, texture, surface diffusion, thermal behavior, fusion, MMC.

Abstract. Thin graded W/Cu coatings plus subsequent heat treatment at 800°C are used to improve the interfacial adhesion between W and Cu. Specimen with ~500 nm thick graded W/Cu coatings were characterized and analyzed after thermal treatment at 550°C, 650°C and 800°C. At 800°C a significant change in the nanostructure is observed. The better adhesion is caused by W/W grain boundary diffusion processes and Oswald ripening of the nanometre-sized grains leading to their interconnection between each other and the W substrate. The phase and texture analysis of graded W/Cu indicates grain growth and diffusion processes of pure W and Cu. The stress analysis shows that the changes in the nanostructure of the W/Cu coatings correlates to the stress relieve of W at temperature starting from 650°C. After cooling of the coating to RT the residue intrinsic tensile stress is caused by thermal mismatches of the substrate and the 100% W layer of the coating.

Introduction

In future fusion reactors like DEMO, the fusion plasma leads to a heat flux of up to 20 MW/m² in the divertor region [1]. Depending on the divertor design, this will lead to high temperatures of up to 550°C at the interface between plasma-facing material (PFM) (W) and water-cooled heat sink material (Cu, CuCrZr)[2]. Metal matrix composites (MMC) like W fiber-reinforced Cu has the potential to strengthen this zone and to improve the mechanical performance at high temperatures compared to conventional Cu-based alloys.

The interfaces between W and Cu occurring within the MMC at the fiber/matrix interface and at the MMC/PFM interface were optimized. Thin graded W/Cu coatings improved the interfacial adhesion between W and Cu. Previous pull-out measurements of single matrix-coated fibers [3] showed that an up to 6 fold increase in shear strength, i.e., a stronger bonding between W fiber and Cu matrix was achieved by depositing a 500 nm thin stepwise graded transition interlayer by magnetron sputter deposition and subsequently additional heat treatment at 800°C. At 800°C W grain boundary diffusion processes were expected resulting in a good bonding between coated W and the W fiber. Additionally, the stepwise graded transition between W fiber and Cu matrix acts as stepwise adaptation of the coefficient mismatch of thermal expansion (CTE) during thermal cycling [3]. Numerous investigations were performed on W/Cu functional graded layers used in fusion application produced by different techniques like powder metallurgy and plasma spraying on mm-scale [4-9]. The here investigated coatings are on nanometer scale and were produced by magnetron sputtering.

To understand the thermal and morphological processes of the 500 nm stepwise graded transition layer due heat treatment during the synthesis of the components and during its use in the divertor, dedicated heating experiments at 550°C, 650°C and 800°C were performed. After each heating step,

planar samples deposited with the stepwise graded coating were investigated regarding its nanostructure by scanning electron microscopy (SEM) and its phase, stress state and texture by X-ray diffraction (XRD) analysis. Moreover, cross-sections of the graded coating deposited on planar W substrates and on W fibers - prepared by focus ion beam analysis (FIB) - were investigated with SEM and with transmission electron microscopy (TEM), respectively, to detect a change in the nanostructure like grain growth and diffusion processes of each layer due to the heating of the samples.

Material and experimental

Thin ~500 nm stepwise graded W/Cu coatings were deposited by magnetron sputter deposition (Discovery 18DC/RF, Denton Vacuum Company) on circular W (Plansee) and SiO_2 (GVB) substrates and on 100 µm thin W fiber (OSRAM). Argon gas was used for sputtering. The Cu concentration is thereby increased in ~25% steps from W to Cu by varying the power to the Cu and W electrodes. Before deposition, the substrates and fibers were etched by the argon plasma for 2 minutes (100 W, 570 V bias) to remove the oxide layer and adsorbed impurities. The substrate holder was rotating with 10 rpm to allow a homogenous deposition and etching. The sample temperature reached 55°C during film deposition. Thereafter the samples were transferred to a vacuum furnace (~$1x10^{-3}$ Pa) and annealed at 550°C, 650°C and 800°C for 60 minutes.

The crystallographic phase analysis, stress state and texture of the planar SiO_2 samples were determined by XRD (XRD 3003 PTS diffractometer, Seifert). A parabolic multilayer mirror was used on the primary side to achieve a parallel beam and K_β suppression. On the secondary side, parallel metal plates, perpendicular to the scattering plane, were installed to restrict the divergences to 0.4°.

The intrinsic stresses were analyzed by XRD using the $\sin^2 \psi$ method. A biaxial residual stress state of rotational symmetry ($\sigma_{13} = \sigma_{23} = \sigma_{33} = 0$ and $\sigma_{11} = \sigma_{22}$) independent of the thickness was assumed for simplification of the complex stress state of the inhomogeneous and textured coating. The thermal stress introduced during the deposition process was calculated using the thermal stress equation [10] and was subtracted from all XRD measured stress values to obtain the intrinsic stresses.

Two scanning electron microscopes (XL 30 ESEM, FEI and Helios Nanolab 600, FEI) were used to analyze the surface morphology and the cross-sections of the planar W samples. A transmission electron microscopy (TEM 1200, JEOL) was applied for the microstructural characterization of the W fiber samples.

Results and discussion

Nanostructure and phase analysis of thin graded W/Cu coating

The microscopic investigation of the initial planar sample by SEM is presented in Figure 1.a). The SEM image of the cross-section obtained by FIB of the stepwise graded W/Cu coating shows clear layers from 100% W to 100% Cu. The grain size differs depending on composition which was measured by Rutherford Backscattering Spectrometry (RBS) and extracted by means of SIMNRA program [11]. After annealing at 650°C the nanostructure of the graded W/Cu coating begins to change slightly. Significant differences in the nanostructure can be seen after annealing at 800°C (see Figure 1.b)). The 100% Cu layer has agglomerated to islands on the surface. This process starts at 650°C. Interconnections between the W of the coating and substrate have been developed after annealing at 800°C. These two effects are caused by surface diffusion and Oswald ripening. During ripening, large grains grow larger at the expense of smaller ones, thus reducing the total surface energy. Energy minimization (Gibbs–Thomson effect) represents the driving force for the

interconnection growth and the diffusive mass transfer between grains is governed by grain boundary diffusion.

Similar effects of the coating are observed on W fiber as on planar samples. The two TEM images (see Figure 1.c) and 1.d)) show the stepwise graded W/Cu coating on W fiber. After annealing at 800°C the same formation of W structure has been build by Oswald ripening as on the planar sample. Additionally, interconnections have been formed between layers and fiber.

The diffraction pattern measured by XRD confirmed that the formed nanostructures by annealing at 800°C are pure W and Cu structures and are not affected by impurities like oxygen. In contrast, the WO_3 (111) peak found in the diffraction pattern of the as-deposited sample has been already removed through thermal heating at 550°C. Oxygen has been incorporated during the deposition process as the increase of the substrate temperature and the argon atom flux make the intra- and the intergranular oxygen diffusion easier [12].

The W (110) diffraction peak (scattering angle 40.26°) was evaluated in respect to the peak width depending on the temperature. The peak width, i.e., the full width at half-maximal (FWHM) value slightly increases from 1.3° in the as-deposited coating to 1.7° after annealing at 550°C. It decreases further to 0.8° after annealing at 650°C and to 0.5° after annealing at 800°C. The decrease should be mainly caused by grain growth by Oswald ripening. Quantitative analysis of the Cu (111) peak width (scattering angle 43.32°) were not possible due to the peak shape asymmetry, which cannot be resolved in the spectra.

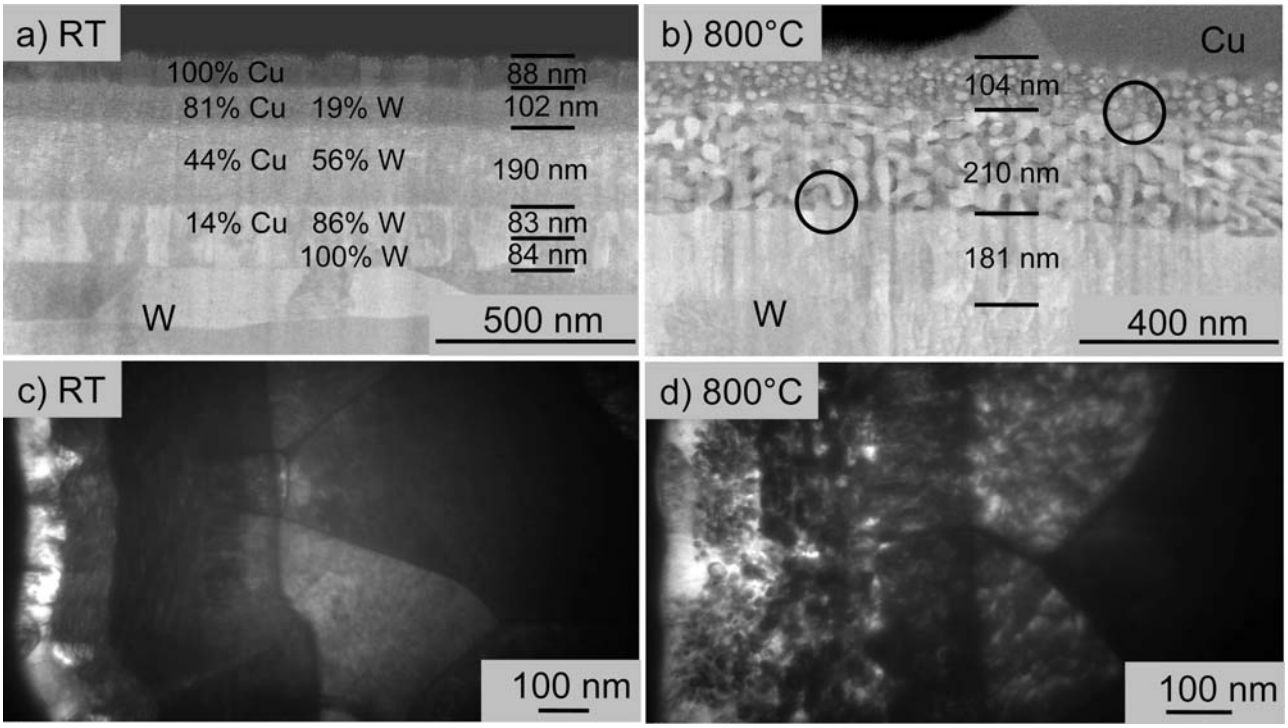

Fig. 1: SEM images of the cross-sections of the stepwise graded W/Cu coating on planar W substrates a) as-deposited with its five layers with thickness and composition designation and b) annealed at 800°C with merged layers and Cu islands on the top. TEM images of the cross-sections of the stepwise graded W/Cu coating on W fiber c) as-deposited and d) annealed at 800°C.

Texture and stress analysis of graded W/Cu coating

After the deposition of the stepwise graded W/Cu coating, W and Cu exhibit a strong fiber texture. A commonly observed texture for fcc metallic films produced by magnetron sputtering - such as Cu - is the {111} fiber texture [13]. This is also the case for the Cu in the coating, as pole figure of the Cu (111) peak demonstrates (scattering angle 43.32°) in Fig. 2.a). The intensities of the diffraction peaks caused by the distribution of crystallite orientations have been recorded depending

on the tilting angles α from 0° to 80° and on the rotation angles β from 0° to 360°. After annealing to 800°C the {111} fiber texture remains. With increasing annealing temperature the (111) peak intensity first decreases and then increases (see Table 1). Interpretations for the decrease have not been found yet, but the increase can be explained by crystallisation of amorphous Cu components and crystallite growth.

W pole figures of the (110) peak (scattering angle 40.26°) are presented as-deposited in Fig. 2.c) and annealed at 800°C in Fig. 2.d). The as-deposited and annealed W of the stepwise graded W/Cu coating is polycrystalline and shows a slightly weaker fiber texture in {110} direction. As already observed for Cu (111), the W (110) peak intensity first decreases and then increases with increasing annealing temperature (see Table 1). Grain growth by Oswald ripening should be primarily responsible for the increase, but also thermally-induced ordering could contribute.

The mosaic spreads, defined as the FWHM value of the tilting scan averaged over 180° rotation, are analyzed for the Cu (111) and for the W (110) texture at RT and after annealing at 550°C, 650° and 800°C (Table 1). The mosaic spread for both phases increases first and then decreases with increasing annealing temperature. The increase of the mosaic spread correlates to the decrease of the intensity of the peaks. The decrease of the peaks is caused by Oswald ripening resulting in an increase of intensity.

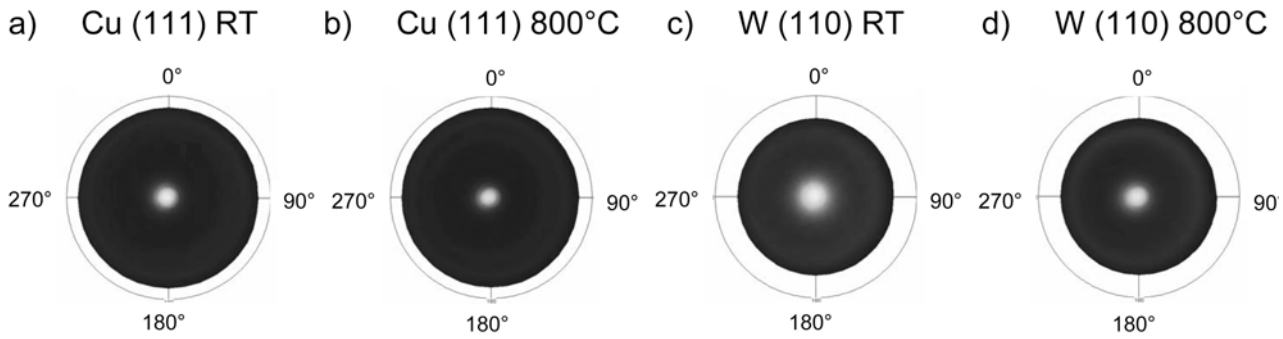

Fig. 2: Pole figures of the Cu (111) peak of the stepwise graded W/Cu coating on planar W substrates a) as-deposited and b) annealed at 800°C. Pole figures of the W (110) peak of the stepwise graded W/Cu coating on planar W substrates c) as-deposited and d) annealed at 800°C.

Cu (111)	Intensity [cps]	Mosaic spread [°]
RT	5931	13.9 ± 0.1
550°C	4470	18.9 ± 0.4
650°C	8506	13.2 ± 0.2
800°C	11393	12.4 ± 0.3
W (110)		
RT	4916	21.8 ± 0.1
550°C	4733	27.4 ± 0.1
650°C	11144	18.4 ± 0.2
800°C	25804	16.2 ± 0.2

Table 1: Overview of the intensity and the mosaic spread of the Cu (111) peak and of the W (110) peak depending on the temperature.

The biaxial residual stress state of rotational symmetry is determined for the thin graded W/Cu coating. Quantitative analysis of the Cu stress state is not possible due to the high Cu {111} fiber texture.

Solely from the analysis of the W (321) peak (scattering angle 131.16°) a tendency regarding the stress state of the W components in the thin graded W/Cu coatings can be concluded. From all measured stress values by XRD, the thermally induced stress of ~0.1 GPa caused by the deposition process is subtracted. An intrinsic tensile stress of ~0.7 ± 0.2 GPa of W is determined in the as-deposited coatings. After annealing at 550°C the intrinsic tensile stress state remains stable (~0.7 ± 0.1 GPa) which correlates to the microscopic investigation showing that the nanostructure of the coating have not been changed.

A clear increase of the intrinsic tensile stress to ~1.5 ± 0.1 GPa after thermal treatment at 650°C and an increase to ~1.8 ± 0.1 GPa at 800°C are determined. At annealing temperatures of ~700°C thermal stresses relieve in W which again correlates with the significant changes in the nanostructure. Regarding this stress relieve, the measured intrinsic tensile stresses after annealing at 650°C and at 800°C are solely caused by thermal induced stresses due to the CTE mismatch of the SiO_2 interface after cooling. It can be assumed that the W-dominated layers of the coating mainly contribute to the stress state. Calculation of the stresses due to the CTE mismatch by using the thermal stress equation [10] verified the interpretation.

As the yield tensile strength (33.3 MPa [14]) of Cu is fare below the stress state of W it can be assumed that the influence of Cu to the stress state of the coating is negligible low.

Conclusion

Significant changes in the nanostructure of thin graded W/Cu coatings have been observed after annealing at 800°C. As expected, the better adhesion between W fibre and Cu matrix by implementing a thin graded transition plus additional heat treatment at 800°C investigated in [3] is caused by W/W grain boundary diffusion processes and Oswald ripening. Interconnections are formed between the layers of the coating and the W substrate. In good agreement to the microscopic investigations, the phase and texture analysis of graded W/Cu indicates grain growth and diffusion processes of pure W and Cu. The stress analysis shows that the changes in the nanostructure of the W/Cu coatings correlates to the stress relieve of W at temperature starting from 650°C. After cooling of the coating to RT, the residue intrinsic tensile stress is caused by thermal mismatches of the substrate and the 100% W layer of the coating. Due to the high sinterability of the nano-sized tungsten, the processing temperature could be lowered close to the expected operation temperature. These results combined with the interfacial adhesion result of the paper [3], show that thin graded W/Cu coatings are suitable as functional and effective interlayer between W and Cu for its use in fusion application.

Acknowledgement

The authors would like to Plansee GmbH (Reutte) for providing the W planar samples and OSRAM GmbH (Schwabmünchen) for providing the W fibers.

A part of this work has been performed within the framework of the Integrated European Project „ExtreMat“ (contract NMP-CT-2004-500253) with financial support by the European Community. It only reflects the view of the authors and the European Community is not liable for any use of the information contained therein.

References

1. Kukushkin, A.S., et al., Fusion Engineering and Design, 2003. **65**(3): p. 355-366.
2. You, J.-H., Journal of Nuclear Materials, 2005. **336**(1): p. 97-109.

3. Herrmann, A., Schmid, K., Balden, M., Bolt, H., Journal of Nuclear Materials, 2008.
4. Pintsuk, G., et al., Fusion Engineering and Design, 22nd Symposium on Fusion Technology, 2003. **66-68**: p. 237-240.
5. Chong, F.L., J.L. Chen, and J.G. Li, Journal of Nuclear Materials Plasma-Surface Interactions-17, 2007. **363-365**: p. 1201-1205.
6. Shen, W.-p., et al., Journal of Nuclear Materials, Proceedings of the Twelfth International Conference on Fusion Reactor Materials (ICFRM-12), Proceedings of the Twelfth International Conference on Fusion Reactor Materials (ICFRM-12), 2007. **367-370**(Part 2): p. 1449-1452.
7. Ge, C.-C., et al., Journal of Nuclear Materials, 9th Int. Conf. on Fusion Reactor Materials, 2000. **283-287**(Part 2): p. 1116-1120.
8. Itoh, Y., M. Takahashi, and H. Takano, Fusion Engineering and Design, 1996. **31**(4): p. 279-289.
9. Davis, J.W., et al., Journal of Nuclear Materials, 1996. **233-237**(Part 1): p. 604-608.
10. Aite, K.H., J.; Middelhoek, J.; Koekoek, R., Material Research Society. 1989.
11. Mayer, M., Tech. Rep. IPP 9/113 Max-Planck-Institut für Plasmaphysik, 1997.
12. Villain, P., et al., Journal of Vacuum Science & Technology A, 2003. **21**(4): p. 967-972.
13. Le Bourhis, E., et al., Plasma Processes and Polymers, 2007. **4**(3): p. 311-317.
14. MatWeb, *Online Material Data Sheet*. 2008.